H-bonded anion-anion complex trapped in a squaramido-based receptor

Rafel Prohens',[*,a] Anna Portell,[a] Mercè Font-Bardia,[b] Antonio Bauzá,[c] and Antonio Frontera[*,c]

a.Unitat de Polimorfisme i Calorimetria, Centres Científics i Tecnològics, Universitat de Barcelona, Baldiri Reixac 10, 08028 Barcelona, Spain. E-mail: rafel@ccit.ub.edu.

b.Unitat de Difracció de Raigs X, Centres Científics i Tecnològics, Universitat de Barcelona.

c. Departament de Química, Universitat de les Illes Balears, Crta. de Valldemossa km 7.5, 07122 Palma (Baleares), Spain. E-mail: toni.frontera@uib.es.

ABSTRACT:

Herein we report the experimental observation (X-ray characterization) of an anion–anion complex (anion = hydrogen fumarate) stabilized by H-bonds that is trapped in a secondary squaramide receptor. High level ab initio calculations indicate that the anion-anion complex is thermodynamically unstable but kinetically stable with respect to the isolated anions design of supramolecular synthons for generating interesting and novel assemblies in the solid state.6 Actually, the utilization of squarate salts is common in crystal engineering7 and organic material research.8 Moreover, secondary squaramides have been used in molecular recognition and supramolecular chemistry due to their strong ability to establish H-bonding interactions both as donors and acceptors.9-11

Theoretical studies have suggested the possibility of finding anion–anion hydrogen-bonded cluster minima in the absence of solvent.1 The existence of a dissociation barrier makes these minima stable, although their overall binding energy is repulsive.1c,d Obviously, the Coulombic energy dominates an interaction that is repulsive in the case of systems with the same charge. The analysis of reported minima structures in hydrogen bonded systems indicates that attractive electrostatic contributions between the groups involved in the HB interaction are the responsible for the presence of such minima.2 Anion-anion repulsion is stronger than hydrogen bonding at long distances. However, at hydrogen bond distances, upon formation of the anti-electrostatic assembly, the complex is kinetically stable. For instance, in phosphate aggregates, the dissociation barrier can be as large as ~17 kcal/mol.1b,c In fact, dimerization of phosphates occurs in near-saturated solutions.3 Furthermore, it has been reported that hydrogen oxalate form hydrogen bonded chains in the solid state. 4 It has been recently shown that the molecular recognition of anions offers the possibility to create capsules containing two guest molecules, i.e. "H–G–G–H" (H = host, G = guest).5 In case the guest is an anion, this strategy gives the opportunity to investigate and characterize anion···anion non-covalent interactions.

Squaramides (squaric acid amides) have been used in the design of supramolecular synthons for enerating interesting and novel assemblies in the solid state.6 Actually, the utilization of squarate salts is common in crystal engineering7 and organic material research.8 Moreover, secondary squaramides have been used in molecular recognition and supramolecular chemistry due to their strong ability to establish H-bonding interactions both as donors and acceptors.9-11

Taking advantage of our previous experience in the synthesis and X-ray characterization of squaric acid derivatives and their utilization in molecular recognition,12-14 in the present communication we have envisaged the utilization of a bis-N,Ndimethylaminoethyl secondary squaramide (SQA, see Scheme 1) in combination with fumaric acid to generate supramolecular assemblies with the formation of anion–anion complexes. The ability of secondary squaramides to form the H-bonding pattern shown in Scheme 1b can be used as a driving force for the formation of the assembly. This combined with the presence of the tertiary amine groups facilitate the formation of hydrogen fumarate anions and their H-bonded complexes. The kinetically stability of such anion–anion complexes has been confirmed by means of high level ab initio calculations.

The solid state structure of the hydrogen fumarate salt is shown in Fig. 1a. It is remarkable the presence of channels formed by the secondary squaramide moieties interconnected by H-bonds. These channels are of adequate size and shape to accommodate two infinite self-interacting chains of hydrogen fumarate anions (see Fig. 1b). The anions also interact with the walls of the channels by means of ion-pair interactions as further described below.

As aforementioned, the theoretical study has been focused on the analysis of the anti-electrostatic H-bonds that are established between the hydrogen fumarate anions. We have computed (see ESI for details) the interaction energies using high level ab initio calculations (RI-MP2/aug-cc-pVTZ level of theory). Fig. 2 shows the optimized geometries of three different anion-anion complexes that are true

minima in the potential energy surface (PES). Their interaction energies are also indicated in the figure. The double “head-to-tail” binding mode leads to the most stable anion–anion complex that is 6.3 kcal/mol higher in energy that the separated monomers. The head-to-head complex is only 1.2 kcal/mol less favored that the double “head-to-tail” binding mode. This is likely due to the presence of two secondary C–H···O interactions in the latter (see blue dashed lines). Finally, we have found another anion–anion complex that is very high in energy (+26.0 kcal/mol), denoted as “head to tail”, where only one strong O– H···O– H-bond is established. Only this binding mode is well suited for the formation of chains since the other two are selfassembled dimers.

The existence of a metastable structure with positive interaction energy values is only possible if a local minimum is present in the PES together with a concomitant dissociation barrier that prevents the monomers to spontaneously dissociate. The dissociation scan plot for the “head-to-tail” binding mode is shown in Fig. 3 and evidences the existence of a 6.2 kcal/mol energetic barrier. Interestingly, the O···H distance in the TS is very long (3.206 Å). At O···H distances longer than 4.5 Å the H-bond is completely broken and the dissociation path converges to the imaginary curve (red dashed line) that corresponds to the potential energy of two isolated negative point charges located at the position of the carboxylate groups. At distances shorter than 4.5 Å the dissociation path and the local minimum are situated well below this imaginary curve.

A detail of the anion–anion interaction observed in the solid state of 1 is given in Fig. 4. It is worth mentioning that, unexpectedly, the charged N+–H group is not pointing to the anionic moiety of the hydrogen fumarate, instead it forms a hydrogen bond with the neutral carboxylic group (O···H distance 1.78 Å). The H-bond distance of the anion–anion complex is 1.65 Å (see Fig. 4b) that is in good agreement with the theoretical one (1.60 Å, see Fig 2c). Moreover, the experimental complex also reveals the existence of the predicted complementary C–H···O interaction (2.38 Å).

We have also studied the anion–anion complex and also the whole assembly including the counter-cation energetically. We have evaluated both the anion–anion and cation–cation complexes as they stand in the X-ray structure. The interaction enrgies are, as expected repulsive (+34.9 for the cation–cation and +37.0 kcal/mol for the anion-anion). We have also computed the interaction energy of the whole assembly (C–A–A–C, C = cation, A = anion), that is large and favorable (ΔE3 = – 29.5 kcal/mol). This interaction energy has been computed considering that the assembly is a binary system (i.e. 2 x C–A→ C–A····A–C).

Finally, we have also performed the AIM analysis of C–A····A–Cassembly, where the anti-electrostatic H-bonding (AEHB) interaction is established. The presence of a bond critical point (CP) and bond path connecting two atoms is an unambiguous evidence of interaction.15 Fig. 6 depicts the AIM analysis of the assembly that reveals an intricate distribution of bond CPs and bond paths due to the existence of a high number of interactions between the anionic and the cationic parts of the assembly. A close look to the distribution (see highlighted area in Fig. 6, right) reveals the existence of a bond CP and bond path connecting the O atom of the carboxylate group to the H atom of the carboxylic group, thus confirming

the existence of the AEHB interaction. More importantly, the O–H···O HB lies exactly above the four membered ring of the squaramide, establishing cooperative lp–π and anion–π (A–π) interactions as revealed by the presence of two bond CPs and bond paths connecting the O atoms to the C atoms of the four membered ring. These secondary O···C interactions confer an extra stabilization to the AEHB.

In conclusion, we have reported the X-ray structure of an anion–anion complex stabilized by H-bonds and a combination of anion/lp–π interactions that is trapped between two secondary squaramide receptors. High level ab initio calculations show that the anion-anion complex is thermodynamically unstable but kinetically stable with respect to the isolated anions. Since carboxylate anions are very common in chemistry, we anticipate that the results published herein may guide other researchers to interpret structural data where carboxylate anions are involved in anion···anion structurally determinant interactions and help chemists to design new multicomponent crystals based on this interaction.

Financial support from the MINECO of Spain (CTQ2014-57393-C2-1-P, FEDER funds) is gratefully acknowledged.

.

NOTES AND REFERENCES

§ Procedure for the preparation of crystals of 1 suitable for X-ray crystallography: See Table S1. ‡ Crystal data for 1 (CCDC no. 1588700): Empirical formula C33H59N8O16, M = 823.88, triclinic, a = 6.196(8) Å, b = 13.132(11) Å, c = 13.815(13) Å, α = 73.83(5) º, β = 83.92(6) º, γ = 78.69(6)º, V = 1057.1(19) Å3, T = 293(2) K, space group P$\bar{1}$, Z = 1, 6197 Reflections measured, 6189 Independent reflections [R(int) = 0.0411], Completeness to θ = 25.003° (99.8 %), Final R indices [I>2σ(I)] were R1 = 0.1770 (all data), wR2 = 0.2466 (all data). See Table S1 for full details

1 (a) F. Weinhold, Angew. Chem. Int. Ed., 2017, 56, 14577-14581; (b) T. J. Mooibroek, CrystEngComm, 2017, 19, 4485-4488; (c) A. Bauzá, A. Frontera and T. J. Mooibroek, Nature Commun., 2017, 8, 14522; (d) A. Bauza, A. Frontera, T. J. Mooibroek and J. Reedijk, CrystEngComm, 2015, 17, 3768– 3771; (e) S. R. Kass, J. Am. Chem. Soc. 2005, 127, 13098 – 13099; (f) I. Mata, I. Alkorta, E. Molins and E. Espinosa, ChemPhysChem, 2012, 13, 1421 – 1424; (g) I. Mata, I. Alkorta, E. Molins and E. Espinosa, Chem. Phys. Lett., 2013, 555, 106 – 109; (h) F. Weinhold and R. A. Klein, Angew. Chem. Int. Ed., 2014, 53, 11214 – 11217; (d) I. Mata, E. Molins, I. Alkorta, E. Espinosa, J. Phys. Chem. A, 2015, 119, 183–194.

2 (a) G. Frenking and G. F. Caramori, Angew. Chem., Int. Ed., 2015, 54, 2596–2599; (b) I. Alkorta, I. Mata, E. Molins and E. Espinosa, Chem.– Eur. J., 2016, 22, 9226–9234.

3 M. K. Cerreta and K. A. Berglund, J. Cryst. Growth 1987, 84, 577−588.

4 (a) M. Mascal, C. E. Marjo and A. J. Blake, Chem. Commun., 2000, 1591−1592. (b) P. Macchi, B. B. Iversen, A. Sironi, B. C.; Chakoumakos and F. K. Larsen, Angew. Chem., Int. Ed., 2000, 39, 2719−2721 (c) T. Steiner, Chem. Commun. 1999, 2299−2300. (d) D. Braga, F. Grepionia and J. J. Novoa, Chem. Commun., 1998, 1959−1960.

5 (a) E. M. Fatila, E. B. Twum, A. Sengupta, M. Pink, J. A. Karty, K. Raghavachari and A. H. Flood, Angew. Chem., Int. Ed., 2016, 55, 14057–14062; (b) L. González, F. Zapata, A. Caballero, P. Molina, C. Ramírez de Arellano, I. Alkorta and J. Elguero, Chem. Eur. J., 2016, 22, 7533.

6 (a) R. Prohens, A. Portell, M. Font-Bardia, A. Bauzá and A. Frontera, CrystEngComm., 2017, 19, 3071-3077; (b) A. Portell and R. Prohens, Cryst. Growth Des., 2014, 14, 397–400; (c) A. Portell, X. Alcobe, L. M. Lawson Daku, R. Cerny and R. Prohens, Powder Diffr., 2013, 28, S470–S480; (c) R. Prohens, A. Portell and X. Alcobe, Cryst. Growth Des., 2012, 12, 4548–4553.

7 (a) T. Kolev, R. W. Seidel, H. Mayer-Figge, M. Spiteller, W. S. Sheldrick and B. B. Koleva, Spectrochim. Acta, Part A, 2009, 72, 502–509; (b) T. Kolev, H. Mayer-Figge, R. W. Seidel, W. S. Sheldrick, M. Spiteller and B. B. Koleva, J. Mol. Struct., 2009, 919, 246–254; (c) B. Ivanova

and M. Spiteller, Spectrochim. Acta, Part A, 2010, 77, 849–855; (d) S. L. Georgopoulos, H. G. M. Edwards and L. F. C. De Oliveira, Spectrochim. Acta, Part A, 2013, 111, 54–61.

8 (a) C. Qin, Y. Numata, S. Zhang, X. Yang, A. Islam, K. Zhang, H. Chen and L. Han, Adv. Funct. Mater., 2014, 24, 3059–3066; (b) Z. Dega-Szafran, G. Dutkiewicz and Z. Kosturkiewicz, J. Mol. Struct., 2012, 1029, 28–34; (c) P. Barczyński, Z. Dega- Szafran, A. Katrusiak and M. Szafran, J. Mol. Struct., 2012, 1018, 28–34.

9 (a) S. J. Edwards, H. Valkenier, Dr. N. Busschaert, P. A. Gale and A. P. Davis, Angew. Chem. Int. Ed., 2015, 54, 4592-4596; (b) N. Busschaert, I. L. Kirby, S. Young, S. J. Coles, P. N. Horton, M. E. Light and P. A. Gale, Angew. Chem. Int. Ed., 2012, 51, 4426-4430; (c) V. Amendola, L. Fabbrizzi and L. Mosca, Chem. Soc. Rev., 2010, 39, 3889-3915; (d) A. Frontera, P. M. Deyà, D. Quiñonero, C. Garau, P. Ballester and A. Costa, Chem. – Eur. J., 2002, 8, 433–438.

10 (a) D. Enders, U. Kaya, P. Chauhan, D. Hack, K. Deckers, R.Puttreddy and K. Rissanen, Chem. Commun., 2016, 52, 1669–1672; (b) A. S. Kumar, T. P. Reddy, R. Madhavachary and D. B. Ramachary, Org. Biomol. Chem., 2016, 14, 5494–5499; (c) D. Zhou, Z. Huang, X. Yu, X. Y. Wang, J. Li, W. Wang and H. Xie, Org. Lett., 2015, 17, 5554–5557; (d) L. Chen, Z.-J. Wu, M.-L. Zhang, D.-F. Yue, X.-M. Zhang, X.-Y. Xu and W.-C. Yuan, J. Org. Chem., 2015, 80, 12668–12675; (e) B. Shan, Y. Liu, R. Shi, S. Jin, L. Li, S. Chen and Q. Shu, RSC Adv., 2015, 5, 96665–96669; (f) M.-X. Zhao, H.-K. Zhu, T.-L. Dai and M. Shi, J. Org. Chem., 2015, 80, 11330–11338; (g) J. Peng, B.-L. Zhao and D.-M. Du, Adv. Synth. Catal., 2015, 357, 3639–3647; (h) W. Sun, L. Hong, G. Zhu, Z. Wang, X. Wei, J. Ni and R. Wang, Org. Lett., 2014, 16, 544; (i) X.-B. Wang, T.-Z. Li, F. Sha and X.-Y. Wu, Eur. J. Org. Chem., 2014, 739; (j) V. Kumar and S. Mukherjee, Chem. Commun., 2013, 49, 11203–11205; (k) K. S. Yang, A. E. Nibbs, Y. E. Turkmen and V. H. Rawal, J. Am. Chem. Soc., 2013, 135, 16050–16053; (l) P. Kasaplar, C. Rodriguez-Escrich and M. A. Pericas, Org. Lett., 2013, 15, 3498–3501; (m) P. Kasaplar, P. Riente, C. Hartmann and M. A. Pericas, Adv. Synth. Catal., 2012, 354, 2905–2910.

11 (a) R. B. P. Elmes, P. Turner and K. A. Jolliffe, Org. Lett., 2013, 15, 5638–5641; (b) K. Bera and I. N. N. Namboothiri, Chem. Commun., 2013, 49, 10632–10634; (c) C. Jin, M. Zhang, L. Wu, Y. Guan, Y. Pan, J. Jiang, C. Lin and L. Wang, Chem. Commun., 2013, 49, 2025–2027; (d) C. Lopez, E. Sanna, L. Carreras, M. Vega, C. Rotger and A. Costa, Chem. – Eur. J., 2013, 8, 84–87; (e) B. Soberats, L. Martinez, E. Sanna, A. Sampedro, C. Rotger and A. Costa, Chem. – Eur. J., 2012, 18, 7533–7542; (f) V. Amendola, L. Fabbrizzi, L. Mosca and F.-P. Schmidtchen, Chem. – Eur. J., 2011, 17, 5972; (g) S. Tomas, R. Prohens, G. Deslongchamps, P. Ballester and A. Costa, Angew. Chem., Int. Ed., 1999, 38, 2208–2211.

12 (a) A. Portell, M. Font-Bardia and R. Prohens, Cryst. Growth Des., 2013, 13, 4200–4203. (b) R. Prohens, A. Portell, M. Font-Bardia, A. Bauzá and A. Frontera, Cryst. Growth Des., 2014, 14, 2578–2587.

13 R. Prohens, A. Portell, M. Font-Bardia, A. Bauzá and A. Frontera, CrystEngComm, 2016, 18, 6437-6443.

14 R. Prohens, S. Tomas, J. Morey, P. M. Deya, P. Ballester and A. Costa, Tetrahedron Lett., 1998, 39, 1063–1066.

15 R. F. W. Bader, Chem. Rev. 1991, 91, 893–928.

We report the experimental observation (X-ray characterization) of an anion–anion complex (anion = hydrogen fumarate) stabilized by H-bonds that is trapped in a secondary squaramide receptor.

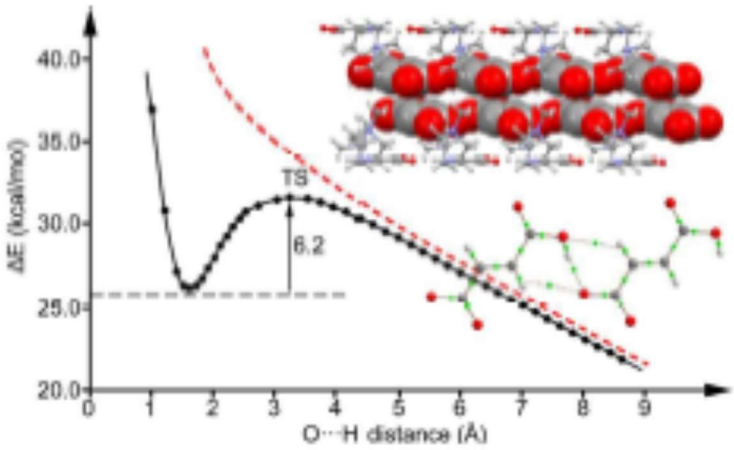

Legends to figures

Scheme 1. (a) Structure of compound 1. (b) H-bonding pattern typical for secondary disquaramides. (c) Cartoon representation of the SQA···A···A···SQA assembly.

Figure. 1 (a) Detail of the channels that are formed in the crystal structure of 1. (b) Detail of the hydrogen fumarate chains (in spacefill format) inside the channel formed by the H-bonded secondary squaramides.

Figure. 2 Three different binding modes for the anion-anion complexes: "head-to-head" (a), double "head-to-tail" (b) and "head-to-tail" (c). Distances in Å.

Figure. 3 Dissociation path of the "head-to-tail" anionic complex in the gas phase. ΔE and d(O-H) stand for the interaction energy and the distance between the H and O atoms, respectively. Red dashed line corresponds to the potential energy curve of two isolated negative point charges located at the position of the carboxylate groups.

Figure. 4 (a) Symmetry equivalence representation of the X-ray structure of 1. (b) Detail of the anion–anion complex between the hydrogen fumarate molecules. Distances in Å..

Figure. 5 Interaction energies of the cation···cation (C–C) complex (a) anion···anion (A–A) complex (b) and C–A····A–C assembly (c). Distances in Å.

Figure. 6 Distribution of bond critical points (CPs, green spheres) and bond paths connecting them. The intramolecular bond CPs and bond paths have been omitted for clarity.

SCHEME 1

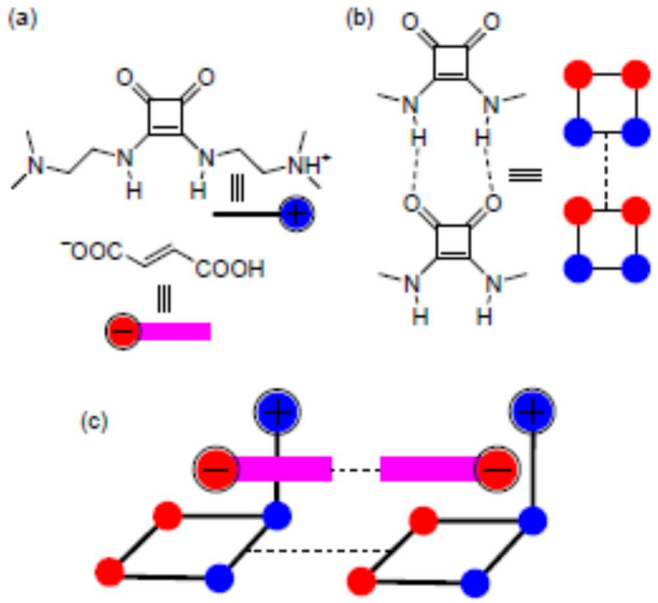

FIGURE 1

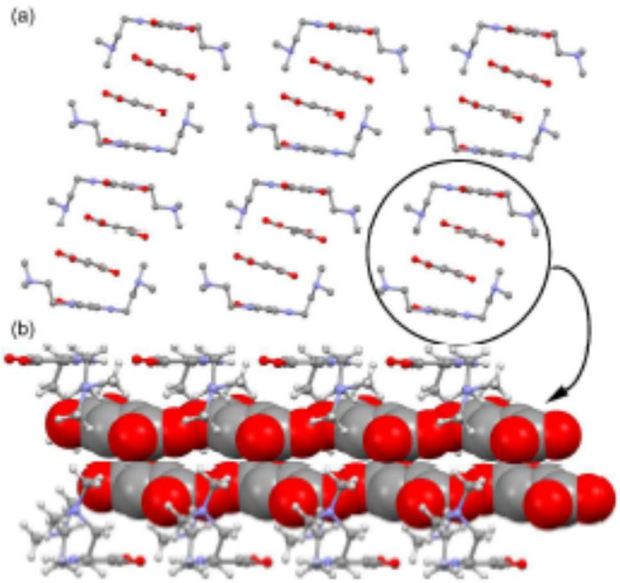

FIGURE 2

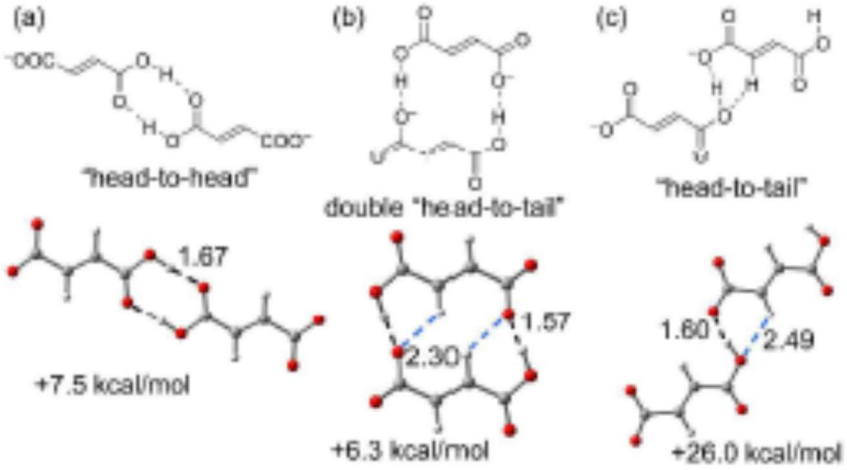
(a)
"head-to-head"
1.67
+7.5 kcal/mol
(b)
double "head-to-tail"
1.57
2.30
+6.3 kcal/mol
(c)
"head-to-tail"
1.60
2.49
+26.0 kcal/mol

FIGURE 3

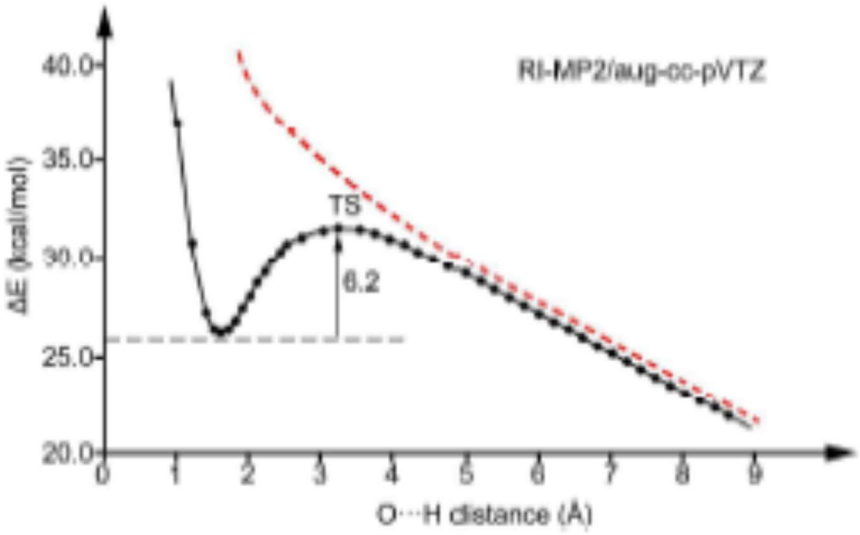
RI-MP2/aug-cc-pVTZ
TS
6.2
ΔE (kcal/mol)
40.0
35.0
30.0
25.0
20.0
0
1
2
3
4
5
6
7
8
9
O···H distance (Å)

FIGURE 4

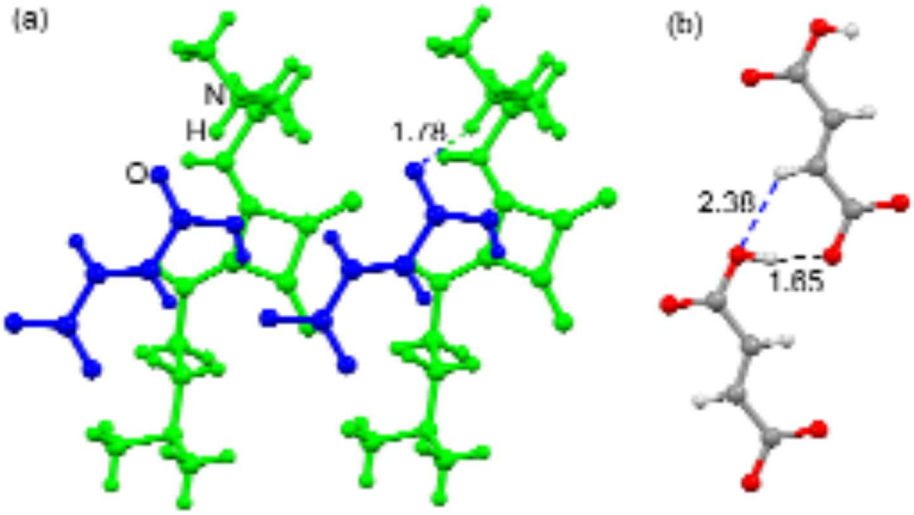

FIGURE 5

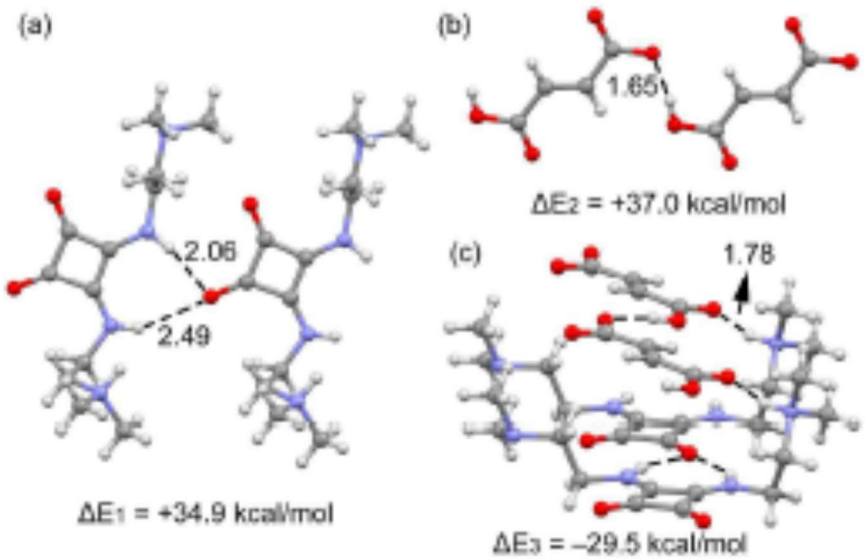
(a)
2.06
2.49
ΔE1 = +34.9 kcal/mol
(b)
1.65
ΔE2 = +37.0 kcal/mol
(c)
1.78
ΔE3 = –29.5 kcal/mol

FIGURE 6